New Anion Exchanger Organic–Inorganic Hybrid Materials and Membranes from a Copolymer of Glycidylmethacrylate and γ-Methacryloxypropyl Trimethoxy Silane

Yonghui Wu,[1] Cuiming Wu,[1] Ming Gong,[2] Tongwen Xu[1]

[1]*Laboratory of Functional Membrane, School of Chemistry and Material Science, University of Science and Technology of China, Hefei 230026, People's Republic of China*
[2]*Laboratory for Materials Behavior and Design, University of Science and Technology of China, Chinese Academy of Science, Hefei 230026, People's Republic of China*

Received 22 March 2006; accepted 4 June 2006
DOI 10.1002/app.24872
Published online in Wiley InterScience (www.interscience.wiley.com).

ABSTRACT: Organic–inorganic hybrid materials and membranes were prepared through coating on Teflon plate or dip-coating on microporous alumina substrates with the solution of glycidylmethacrylate (GMA) and γ-methacryloxypropyl trimethoxy silane (γ-MPS) copolymer, followed by ring-opening of the GMA moiety with trimethylamine hydrochloric and sol–gel reaction of the γ-MPS moiety. Composition of the GMA and γ-MPS copolymer was varied by changing the feed ratio of GMA to γ-MPS during the copolymerization. So the thermal stability, hydrophilicity, electrical properties, etc. of the hybrid materials and membranes were varied. Results showed that as the γ-MPS amount increased in the copolymer, T_d (the temperature on thermogram at 5% weight loss) value of the hybrid materials and water contact angle of the hybrid membrane generally increased, while the anion exchange capacity, water uptake (W_R) and pure water flux decreased. The charge transition point of the hybrid membranes deduced from their streaming potential behavior decreased from pH > 12 to pH = 7–8 as the γ-MPS amount increased. © 2006 Wiley Periodicals, Inc. J Appl Polym Sci 102: 3580–3589, 2006

Key words: organic–inorganic hybrid membranes; anion exchange membranes; sol–gel; γ-methacryloxypropyl trimethoxy silane; glycidylmethacrylate

INTRODUCTION

Hybrid organic–inorganic materials prepared by the sol–gel process have been the subjects of a large number of researches over the past decade, due to their unique feature of combining the properties of traditional materials.[1–5] It was observed that during the preparation process, formation of covalent bonding between organic polymers and inorganic components contributes to the enhancement of the compatibility in the hybrid materials. One route for forming such covalently connected hybrids is to couple organically modified alkoxysilane to organic polymer backbone. The obtained polymers contain pending or terminal trialkoxysilyl groups, so they can undertake hydrolysis and condensation processes afterwards to form inorganic SiO_2 network. Polyethylene oxide (PEO)/SiO_2,[6,7] poly(2-hydroxyethyl acrylate-*co*-methyl acrylate)/SiO_2/TiO_2[8] and polyimide/SiO_2[9] hybrids have been prepared through such method. Another route is to copolymerize organic monomers with organically modified alkoxysilanes. The copolymer can then undergo the sol–gel process to produce hybrid materials. For example, styrene or methyl methacrylate was copolymerized with γ-methacryloxypropyl trimethoxy silane (γ-MPS). The obtained copolymer then underwent sol–gel process together with or without inorganic metal alkoxide to form polystyrene (PS)/SiO_2[10] or poly(methyl methacrylate)/SiO_2/TiO_2 hybrids.[11]

With the development of research jobs on organic–inorganic hybrid materials, hybrid membranes have drawn interests of many researchers because they can show remarkably improved mechanical,[12] thermal,[13] and electrical[14] properties of membranes compared with pure organic membranes. Among the many varieties of hybrid membranes, negatively or positively charged membranes are of special interests since they are needed on some important occasions such as polymer electrolyte membrane fuel cells chemical sensors, retention of multivalent ions, and recovery of valuable metals under high temperature,

Correspondence to: T. Xu (twxu@ustc.edu.cn).
Contract grant sponsor: Natural Science Foundation of China; contract grant number: 20576130.
Contract grant sponsor: Special Foundation for Doctoral Discipline of Ministry of Education of China; contract grant number: 20030358061.
Contract grant sponsor: National Basic Research Program of China; contract grant number: 2003CB615700.

acidic or oxidizing environment.[6,7,15,16] So their exploration would be very meaningful and promising.

In our laboratory, there has been some work on charged organic–inorganic hybrid materials and membranes based on introducing inorganic content in the polymer matrix such as PEO,[17–19] poly(methyl acrylate),[20] and poly(2,6-dimethyl-1,4-phenylene oxide) (PPO).[21,22] In these works, the introduction of the inorganic silica content was through the coupling of organically modified alkoxysilane such as *N*-[3-(trimethoxysilyl) propyl] ethylene diamine (A-1120),[17,20] phenylaminomethyl triethoxysilane,[18,19] and 3-aminopropyl-trimethoxy silane[21,22] to the matrix of organic polymer chains, followed by sol–gel process. So the molecular weight of the organic polymer and the ratio of the inorganic and organic component would be relatively fixed.

As has been mentioned, another important route of preparing hybrid material is to copolymerize organic monomers with organically modified alkoxysilane. Through this route, the ratio of the inorganic and organic component can be conveniently adjusted. So hybrid materials or membranes with flexible compositions and properties can be achieved.

In a previous article by Mouanda,[23] glycidylmethacrylate (GMA) as the organic monomer and γ-MPS as the organically modified alkoxysilane were copolymerized. The copolymer was used for the grafting of polyvinylimidazole onto silicon wafers. It was shown that the GMA and γ-MPS copolymer had relatively high thermal stability and good adhesion to inorganic substrates. So in our present article, such copolymer was utilized in another direction, i.e., the preparation of new anion exchange materials and membranes. The epoxy groups, which are contained in the copolymers, were converted to quaternary ammonium groups through reacting with amines and the trimethoxysilyl groups were converted to inorganic silica network through sol–gel process. Characterizations of the obtained hybrid materials and membranes would be fully discussed.

EXPERIMENTAL

Materials

Glycidylmethacrylate (GMA) and γ-methacryloxypropyl trimethoxy silane (γ-MPS) were purchased from Shanghai Chemical Reagent Company (China) and purified by vacuum distillation (∼ 2 mmHg) over hydroquinone at ∼ 95°C and ∼ 130°C, respectively. Azobisisobutyronitrile (AIBN) was dissolved in warm methanol (35°C), recrystallized in an ice bath, and then dried in a vacuum oven at room temperature. Toluene, *n*-hexane, and ethanol were distilled and kept in molecular sieve before use. Other reagents were used as received.

Asymmetrical microporous α-alumina substrates, with a thin top Al_2O_3 layer (average pore size about 0.4–0.5 μm) and a support ceramic layer (average pore size about 1 μm), were commercially obtained from Institute for Ceramic Research in ZiBo (Shandong, China). Total thickness of the alumina substrates was around 0.36 cm.

Trimethylamine hydrochloride was prepared from the reaction of trimethylamine and hydrochloric acid at 80–90°C. Molar ratio of trimethylamine and hydrochloric acid was 1 : 1 and the reaction continued for 30–40 min.

Preparation of the GMA and γ-MPS copolymer

The copolymer of GMA and γ-MPS was prepared through the free radical polymerization.[23] The copolymerization was carried out in dry toluene solution (0.1 mol GMA and γ-MPS in 70 mL toluene) under argon atmosphere. AIBN (0.2 mol %) was used as initiator and the reaction solution was stirred at 70°C for 24 h. The obtained copolymer was purified by toluene dissolution/hexane precipitation and washing for several times. Pure and dry copolymer was obtained by drying at 30°C under vacuum. Feed ratio (GMA/γ-MPS) were varied from 80/20, 70/30, 50/50 to 30/70 and the obtained copolymers were signified as copolymer A, B, C, D, respectively.

The copolymerization route was shown in Scheme 1.

Preparation of the hybrid materials and membranes

The preparation of the hybrid membranes included three steps. The first was the dip-coating step: The copolymer was dissolved in toluene to obtain 30% (w/v) coating solution. Into the coating solution, the microporous α-alumina substrate was dipped for around 10 s. The dip-coated substrate was air-dried at room temperature overnight, heated from 60°C to 127°C at the rate of 15°C/h and kept at 127°C for 2 h.

The second step was the ring-opening reaction step. The dip-coated substrate was immersed in the ethanol solution of trimethylamine hydrochloride (35 g/L) at 75°C for 2 h. Then the substrate was washed with ethanol for several times to get rid of the remaining trimethylamine hydrochloride.

The third step was the sol–gel reaction step. The substrate, which had undertaken the former two steps, was immersed in the solution of excessive ethanol (∼ 25 mL) and acidic water(∼ 25 mL) at 75°C for 0.5 h. The pH of the acidic water was adjusted to be 5 by hydrochloric acid. Then the substrate was taken out, heated from 60°C to 127°C at the rate of 15°C/h, and kept at 127°C for 2 h to finish the sol–gel reaction.

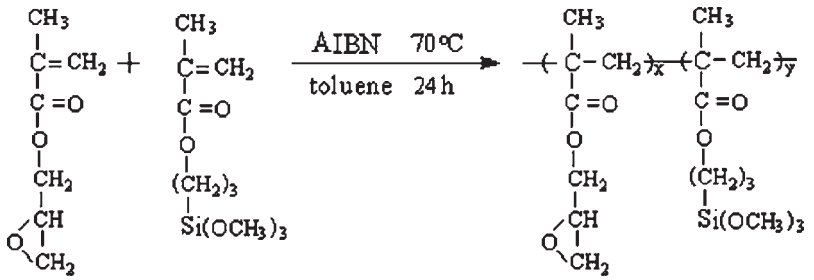

Scheme 1 The copolymerization of GMA and γ-MPS to prepare copolymers A, B, C, and D.

Reactions of the ring-opening and sol–gel processes were shown in Scheme 2.

To increase the thickness of the active layer and to remove any pinholes in the coatings, the above three preparation steps were conducted twice for the same alumina substrate to obtain the final hybrid membrane. Membranes prepared from copolymer A, B, C, and D were signified as membrane A, B, C, and D, respectively.

For the preparation of the hybrid materials, coating solutions of the copolymers A–D were dropped onto teflon plates, dried, and then heated to obtain colorless nonsupported films. The films then underwent the same ring-opening reaction as the hybrid membranes. At the end of the ring-opening process, acidic water was added to the reaction mixture for the same sol–gel process as the hybrid membranes. The obtained powders were washed with water and heated at 127°C for 2 h. Products were correspondingly denominated as hybrid materials A, B, C, and D, respectively.

Characterizations of the hybrid materials

Since the hybrid materials were obtained from the ring-opening and sol–gel processes of copolymers A–D, the chemical structure of the copolymers would be essential to determine the structure of the hybrid materials. To determine the structure of the copolymers, their ^{1}H NMR measurements were conducted on a Bruker DMX-300 NMR instrument operating at 300 Hz. $CDCl_3$ was used as solvent and tetramethylsilane as internal standard.

IR spectra of the hybrid materials A–D were recorded with a Vector 22 Fourier transform infrared spectrometer (Bruker) in a wave-number range from 400 to 4000 cm^{-1}. Samples for IR analysis were prepared at 25°C in the form of KBr pellets.

Thermogravimetric analysis (TGA) of hybrid materials A–D were performed under nitrogen flow on a Shimadzu TGA-50H analyzer. The thermal program was set at a heating rate of 10°C/min. The weight of samples used in all measurements was 5–10 mg.

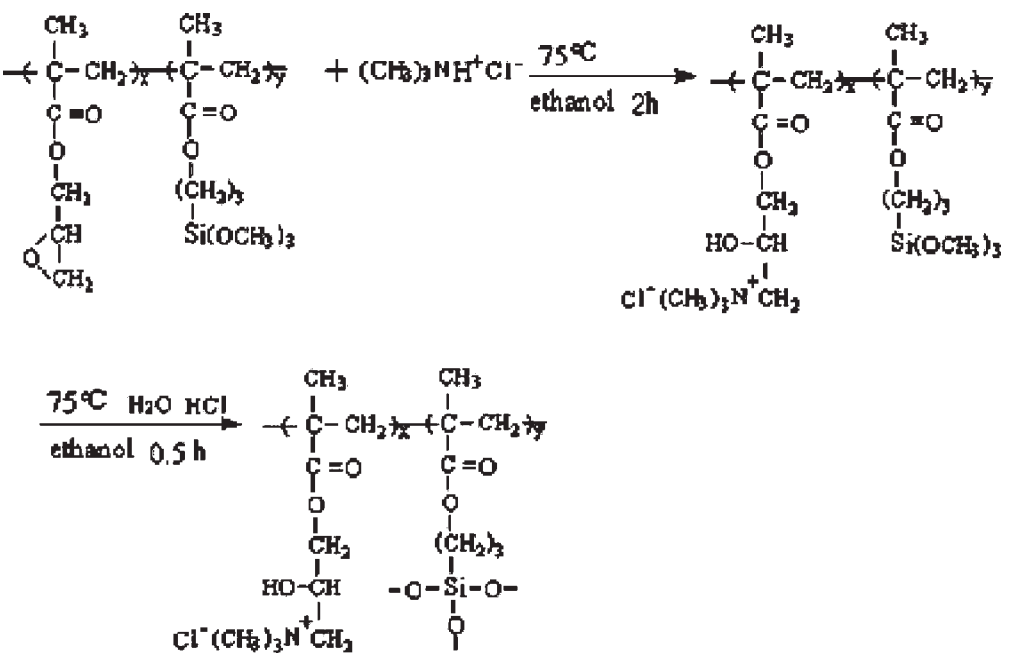

Scheme 2 The ring-opening and sol–gel process of copolymers A, B, C, and D to prepare hybrid materials and membranes A, B, C, and D.

Ion exchange capacities (IEC) of the hybrid materials were carried out as described in our previous article.[20] Accurately weighed dry hybrid materials A–D (within 0.2–1.0 g) were soaked in 200 mL 1.0 mol/L NaCl for 24 h and thus converted to Cl^- ionic form. Then the excessive Cl^- ionic was washed free with deionized water. Afterwards, the hybrid materials were immersed in 200 mL 1.0*M* $NaSO_4$. By deciding the amount of the generated Cl^- with ion-exchange chromatography (DIONEX, DX-120), anion exchange values of the hybrid materials A–D were obtained.

Water content (W_R) was measured as following: The hybrid materials A–D (within 0.2–1.0 g) were dried in a vacuum oven at 80°C until a constant weight was attained. Then they were immersed in ~ 70 mL distilled water at 25°C for 36 h. Since the hybrid materials were powders, they suspended in water and could not be directly taken out. Therefore, the hybrid materials in the distilled water was put on a filter paper and filtered at reduced pressure (~ 400 mmHg) until no water was dripped for around 3 s. Then the hybrid materials were weighed. W_R was calculated as the relative weight gain per gram of the dry hybrid material A–D samples. Every sample was measured for three times to evaluate the reproducibility of this measurement method.

Characterizations of the hybrid membranes

The hydrophilicity of the membranes was characterized by their water contact angles with deionized water using a Model JY-82 contact angle analyzer at 25°C. Fracture surfaces and cross sections of the membranes were gold-coated and examined by environmental scanning electron microscopy using an XL30-ESEM (Philips) instrument.

The unit employed for water flux measurement was the same as that in our previous article.[17,19] The hybrid membranes were placed in a self-made dead-end membrane module. The water flux (F) was calculated as $F = V/At\Delta P$, where V was the total volume of water permeated during the experiment, A represented the membrane area, t denoted the operation time, and ΔP the pressure difference across the membranes.

The unit employed for streaming potential (SP) measurement was the same as that in our previous article.[17,19] We used 0.01*M* KCl as the electrolyte because in aqueous solutions the cations (K^+) and the anions (Cl^-) have equal mobilities.[24] The pH of the KCl solution was regulated from 7 to 13 by adding HCl or KOH solution. During the measurements, the KCl solution was put in the unit by N_2 pressure controlled by a gauge. Reversible Ag/AgCl electrodes, placed on both sides of the membrane, were used to measure the resulting electrical potential difference (ΔE) as the pressure difference across the membrane (ΔP) changed. The area of the membrane exposed to the flow was 4.9 cm^2. SP of the membranes were calculated as $\Delta E/\Delta P$.

RESULTS AND DISCUSSION

^{1}H NMR and FTIR spectra

As mentioned in the experimental section, feed ratio (GMA/γ-MPS) of the copolymers were varied from 80/20, 70/30, 50/50 to 30/70. To decide the chemical structure of the copolymers, ^{1}H NMR spectra of the copolymers were conducted and shown in Figure 1.

In Figure 1, the characteristic proton resonance signals are given according to the report by Mouanda.[23] The main impurity in the copolymers is toluene (~ 7.2 ppm and 2.35 ppm for phenyl and methyl protons, respectively), which was introduced from the precipitation and washing processes. Ratio of the integrated area of the $-Si(OCH_3)_3$ protons signal (3.6 ppm) to $-CH_2-Si$ protons signal (0.65 ppm) is 3.9, 3.6, 3.4, and 4.1 for copolymer A, B, C, and D, respectively. These values are all lower than the theoretical one of 4.5. So it can be deduced that part of the $-Si(OCH_3)_3$ groups have been hydrolyzed during the copolymerization. The copolymer compositions can be estimated from the ratios of the integrated signal of $-CH_2-Si-$ proton to CH proton of epoxy groups and the estimation results are listed in Table I.

For the preparation of the hybrid materials (or membranes), the copolymers A–D underwent ring-

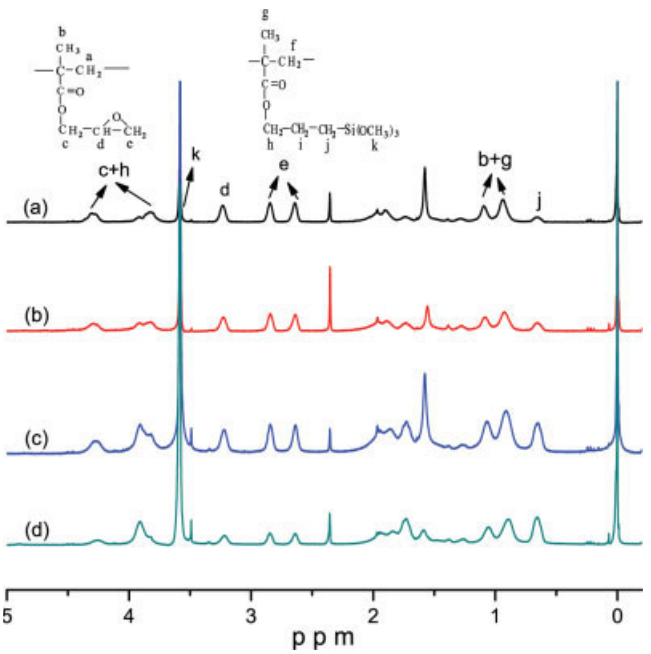

Figure 1 ^{1}H NMR spectra of (a) copolymer A, (b) copolymer B, (c) copolymer C, and (d) copolymer D. [Color figure can be viewed in the online issue, which is available at www.interscience.wiley.com.]

TABLE I
Compositions of the Copolymers A–D and TGA Analysis Results of the Hybrid Materials A–D

Copolymer	Feed ratio (GMA/γ-MPS)	Copolymer compositions (GMA/γ-MPS)[a]	Hybrid material	T_d (°C)[b]
A	80/20	83/17	A	228
B	70/30	71/29	B	223
C	50/50	56/44	C	241
D	30/70	35/65	D	251

[a] Compositions are determined from the ^{1}H NMR spectra of the copolymers.
[b] The thermal degradation temperatures (T_d) are defined as the temperature on thermogram at 5% weight loss.

opening and sol–gel processes. Total yields of the ring-opening and sol–gel processes were 78%, 70%, 81%, and 81% for copolymers A, B, C, and D, respectively. Since the hybrid materials could not be dissolved in usual solvents and solid ^{1}H NMR is not available at this moment, FTIR spectra instead of ^{1}H NMR measurement were conducted and the resulted are shown in Figure 2. All the spectra in Figure 2 show a band at 1732 cm^{-1} specific to the carbonyl stretching vibration in ester ($\nu_{C=O}$)[25] and a large band between 3100 and 3600 cm^{-1}, which is characteristic to the stretching vibration of —OH groups. The —OH groups may be from the ring-opening of the epoxy groups of the copolymers with $N(CH_3)_3H^+Cl^-$ or from the uncondensed —Si—OH groups. However, the absence of the peak at 920–960 cm^{-1} indicates that few —Si—OH groups remain in the hybrid materials. So the hybrid materials were condensed relatively completely and the —OH groups are mainly from the ring-opening of the epoxy groups. The bands observed in the 2800–2990 cm^{-1} region characterize the valence vibration of CH_3—, —CH_2— and CH— structures, while peaks at 1080–1180 cm^{-1} are in the region of C—O—C stretching from esteric structure and —Si—O—Si— stretching.[26]

As has been researched, in FTIR spectrum there should be three bands at 1260 cm^{-1} (ν_{as}), 950–815 cm^{-1} (ν_s), and 760 cm^{-1} (δ), which are associated with the epoxy groups in GMA component.[27] In Figures 2(a)–2(d), the former two bands (1268 cm^{-1}, 914 cm^{-1}) can be observed. However, no band at 760 cm^{-1} exists. So it is likely that few epoxy groups remain in the hybrid materials. The bands at 1260 and 914 cm^{-1} of the hybrid materials may be due to stretching vibrations of C—O bond from esteric structure and the strained siloxane bridge.[28]

Comparing the four spectra in Figure 2, it can be observed that generally, the intensity of the band at 1080–1180 cm^{-1} increases from Figures 2(a) to 2(d) as compared to the band at ~ 1730 cm^{-1}. This is easy to understand: Amount of γ-MPS in the hybrid material increases gradually from hybrid material A–D, so the silica component in the hybrid material increases gradually. On the other hand, number of the ester groups in the hybrid materials is relatively fixed. Thus relative intensity of the C—O—C and —Si—O—Si— stretching bands (1080–1180 cm^{-1}) increases as compared to the C=O stretching vibration in ester (~ 1730 cm^{-1}).

Thermal stability (TGA analysis)

The weight-loss behaviors of the hybrid materials were studied with TGA at a heating rate of 10°C/min in a nitrogen atmosphere. Thermal degradation temperature (T_d; defined as the temperature at 5% weight loss) can be determined from TGA thermograms in Figure 3. The results are summarized in Table I.

From Table I, it can be seen that as the γ-MPS composition increases from hybrid material A to D, T_d value generally increases. Hybrid material A has relatively lower T_d value of 228°C, while hybrid material

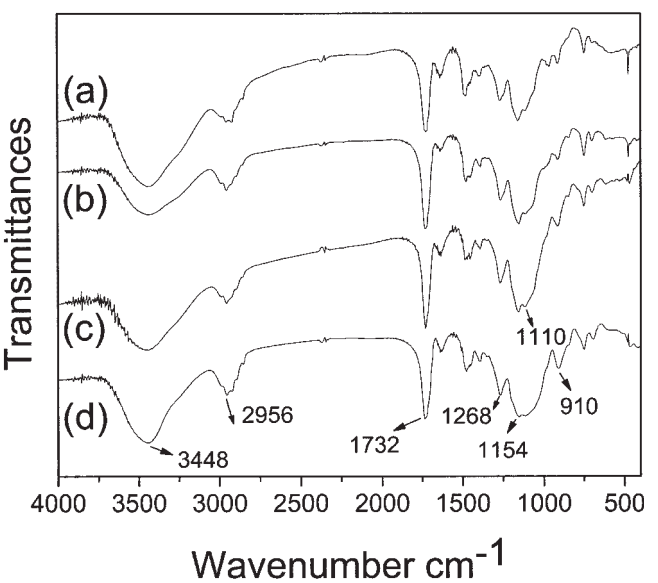

Figure 2 The FTIR spectra of (a) hybrid material A, (b) hybrid material B, (c) hybrid material C, and (d) hybrid material D.

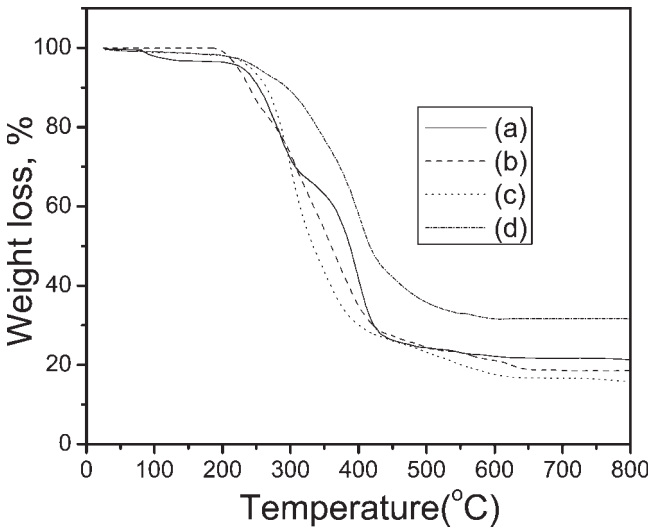

Figure 3 TGA results for (a) hybrid material A, (b) hybrid material B, (c) hybrid material C, and (d) hybrid material D.

C and D has higher T_d value of 241°C and 251°C, respectively. So the thermal stability of the hybrid material generally increases from hybrid material A to D. This is most probably due to the gradually strengthening of the silica network as the γ-MPS composition increases.

Ion-exchange capacity

Anion exchange capacities (IEC) of the hybrid materials A–D were measured and the results were shown in Table II. It can be seen that the IECs of the four kinds of hybrid materials are in the range of 0.83–1.36 mequiv/g, indicating them to be positively charged, i.e., they possess anion-exchange groups. These groups were formed during the ring-opening reaction process of the copolymers with $N^+(CH_3)_3HCl^-$.

It can also be seen from Table II that as the γ-MPS component increases from hybrid material A–D, the IEC decreases gradually. As it was the epoxy groups in GMA that underwent the reaction with $N^+(CH_3)_3HCl^-$ to form the anion-exchange quaternary ammonium groups, it is easy to understand this result. The lower GMA component the copolymer of GMA and γ-MPS contains, the less epoxy groups the copolymer possesses, and thus the less quaternary ammonium groups the hybrid materials possess after the ring-opening and sol–gel process of the copolymer.

Theoretical IEC values of the hybrid materials were also calculated and shown in Table II, assuming complete conversion of the epoxy groups in the GMA moiety to quarteramine (—$N^+(CH_3)_3$—) groups after the ring-opening reaction. It is surprisingly found that the practical IEC values of the hybrid materials are much lower than the theoretical ones. This may be due to the deviation of the actual reaction processes during the hybrid materials preparation from the theoretical ones shown in Scheme 2. For example, during the copolymerization and ring-opening reactions, trace amount of water introduced into the reaction bottle may react with the epoxy groups in the GMA moiety. Also, the quaternization reaction may be incomplete and the remaining epoxy groups may react with water during the sol–gel process or crosslink with each other during the heating process. Another undesirable reaction may be the reaction of the —Si—OH groups with the epoxy groups. As discussed in the above ''^{1}H NMR and FTIR spectra'' section, the —$Si(OCH_3)_3$ groups had been partially hydrolyzed during the copolymerization. The resulted —SiOH might probably participate in the ring-opening of the epoxy groups. These undesirable reactions consumed the epoxy groups in GMA moiety and didn't produce ion exchange groups, thus causing lower IEC values than theoretical values.

Water uptake (W_R) and contact angle

Water uptake of the hybrid materials A–D and water contact angle of the hybrid membranes A–D are listed in Table II. It can be seen that from hybrids A to D, the water uptake gradually decreases while the contact angle increased, indicating that the hydrophilicity gradually decreased. This is in accordance to the gradually decreasing IEC values of the hybrid materials or membranes A to D. Compared with the W_R values in our previous article,[19] the W_R values here are relatively lower while the IEC values relatively

TABLE II
Ion Exchange Capacity (IEC), Water Uptake (W_R), and Water Contact Angle of the Hybrid Materials or Membranes A–D

Hybrid mateirals or membranes	Practical IEC (mequiv/g)	Theoretical IEC (mequiv/g)	W_R (%)	Water contact angle
A	1.36	3.65	141.4 (± 5.2)	83.4°
B	1.10	3.21	134.87 (± 1.5)	84.2°
C	1.00	2.63	82.96 (± 2.4)	87.0°
D	0.83	1.76	79.35 (± 2.2)	88.2°

higher. This is most probably due to the difference in the chemical structure of the hybrid materials. In our previous article,[19] highly hydrophilic PEO polymer chains were used as the organic polymer component in the hybrid material, while in this article, the main polymer chain used was the relatively less hydrophilic polyester.

Morphology of the prepared membranes

To show the structure difference between the substrate and the hybrid membranes, the SEM observations were conducted. It seems that the structure is not affected significantly by the kind of coating solution. Therefore, as examples, the SEM results of membrane D were illustrated here for comparison with those of substrate. As shown in Figure 4(a), micrograph of the alumina substrate displayed some large pores and voids, while in Figure 4(b), the microstructure of the hybrid membrane becomes quite smooth and dense. No obvious pores and voids can be observed. These observations indicated that hybrid films actually formed on alumina substrates through the sol–gel method and the membranes are quite dense.

The cross section SEM of the alumina substrate and membrane D were shown as examples in Figure 4(c, d). In Figure 4(c), a two-layer structure can be observed, while in Figure 4(d), there is a three-layer structure. So in the hybrid membrane, the top dense layer was the hybrid membrane prepared in this article, while the intermediate layer and the bottom one corresponded to a 0.4–0.5 μm Al_2O_3 layer and porous ceramic support, respectively. From this point of view, hybrid membranes with asymmetrical structure were successfully obtained in this article.

Water Flux

Pure water flux through the membranes was tested to explore further the texture of the membranes. For comparison, water flux of the alumina substrate before coating was also measured and the corre-

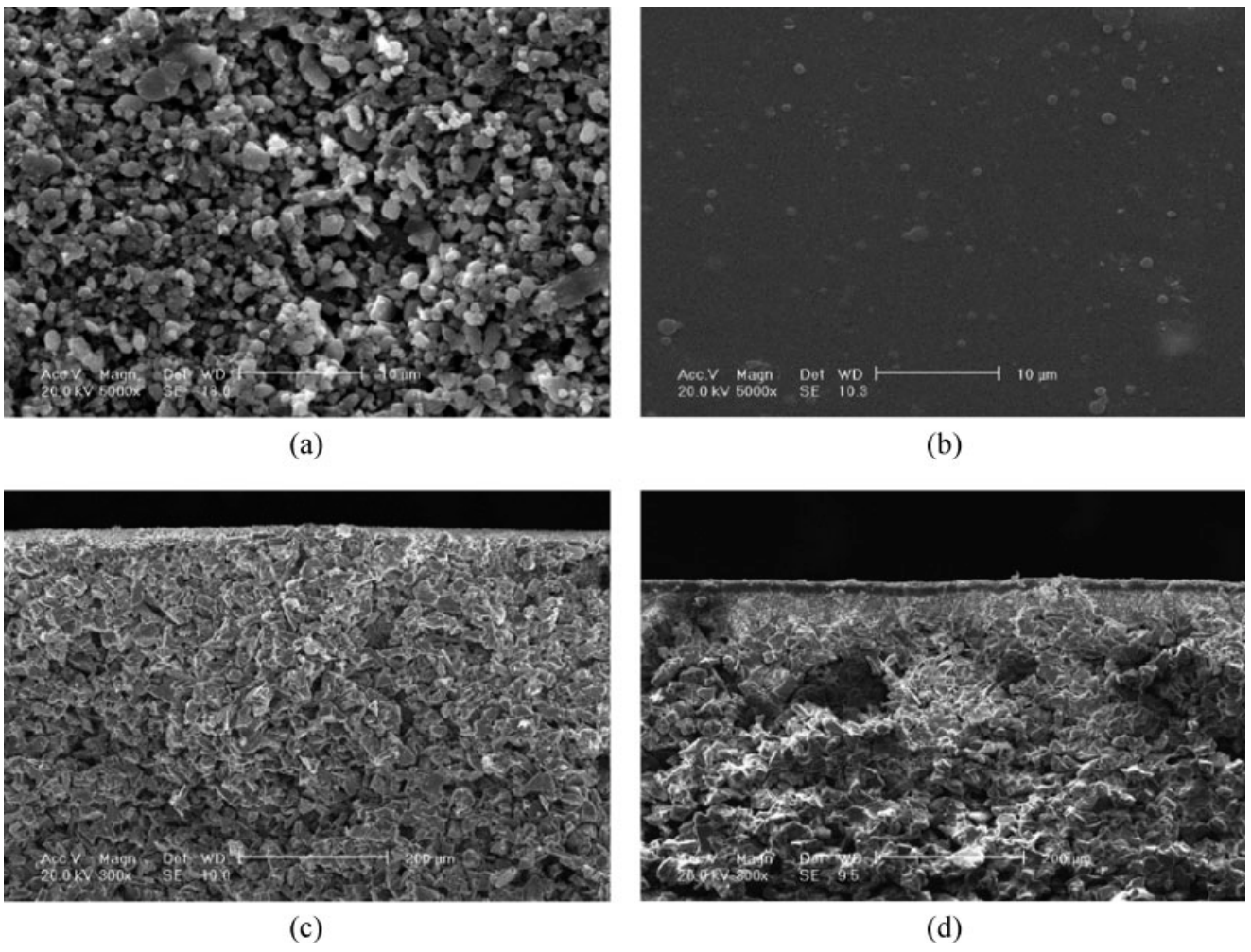

Figure 4 The SEM diagrams of (a) surface of the alumina substrate, (b) surface of membrane D, (c) cross section of the alumina substrate, and (c) cross section of membrane D.

TABLE III
Pure Water Flux (L/(m^2 bar h)) and the Estimated Pore Diameter (μm, Shown in Parentheses) of the Alumina Substrates or Hybrid Membranes A–D after Two Times of Coating

	A	B	C	D
Alumina substrates	10500 (0.53)	5300 (0.38)	7600 (0.45)	9500 (0.50)
Hybrid membranes	1.19 (0.006)	0.51 (0.004)	0.34 (0.003)	0.10 (0.002)

sponding results were shown in Table III. Obviously, water fluxes of the alumina substrates before coating are in the range of 5300–10,500 L/(m^2 bar h). After two times of coating, the membranes water flux dramatically decrease to the range of 1.19–0.10 L/(m^2 bar h). This decrease in the water flux confirms the SEM observation results that dense hybrid membranes were successfully formed on the substrates.

As to the difference in the water flux among membranes A–D, from our previous researches,[17–20] it is known that several factors influence the water flux of a hybrid membrane, including coating time, concentration of the coating solution, structure of the substrate and ion exchange capacity of the membrane. For example, water flux of membranes should increase with the increasing of their IEC values and the substrate pore diameter if there is no blocking of the coating solution in the pores. In this article, coating time and concentration of the coating solution was the same for membranes A–D, so mainly IEC value and the structure of the substrates influence the membrane water flux. From Table III, it can be seen that from membranes A to D, the water flux decreases from 1.19 to 0.10 L/(m^2 bar h). This decreasing trend may be mainly due to the decreasing of IEC values from membranes A to D. For example, for membrane B, though the pore diameter of the substrate is the smallest, the membrane's flux is larger than membranes C and D. On the other hand, for membrane D, its substrate flux is relatively large. However, the membrane's flux is the smallest. So it can be said that among the hybrid membranes A–D, the influence of the IEC value covers the influence of the structure of the substrate and plays main role in determining the membranes flux value.

Applying similar method to that in our previous article,[19] pore sizes of the alumina substrates and the hybrid membranes are estimated from the water fluxes and the results were shown in bracket of Table III. As can be seen, the average pore diameters for the hybrid membranes are in the range of 0.005–0.002 μm, indicating that the charged hybrid membranes with nanometer-structure were obtained.

Streaming potential

The SP measurements were conducted in 0.01*M* KCl solution and started from pH = 7 to pH = 13. It was found that at pH = 7–12, the ΔE values at different pressures were stable and the slope of the $\Delta E - \Delta P$ plot displayed relatively good linearity for each membrane. So the SP value was calculated as $\Delta E/\Delta P$ and the results were shown in Figure 5. However, at pH = 13, the SP measurement became rather difficult since at a given pressure, the E value might vary to a great extent even after quite a long period of time (1–2 h). So we had to give up the SP measurement at pH = 13. To find what might be the reason that caused this abnormity, we changed the pH again to 4, 5, 6, and 7 and conducted the SP measurement for the same membranes. It was found that the membranes behaved similarly as at pH = 13. So long period of time of the membrane's dipping in the KCl solution at pH = 13 must have destroyed the membranes. This is understandable since the alumina substrates and the silsesquioxane network of the hybrid membranes can't stand strong basic solution long.

Similar to our previous articles,[19,29] our measurements of SP here are mainly to find and compare the charge transition point of the membranes A–D if there are any. At pH = 7–12, the charge transition point of the membranes had been successfully found out (as discussed below). So we made no effort to make new hybrid membranes to replace the destroyed ones and conduct the SP measurement at pH lower than 7.

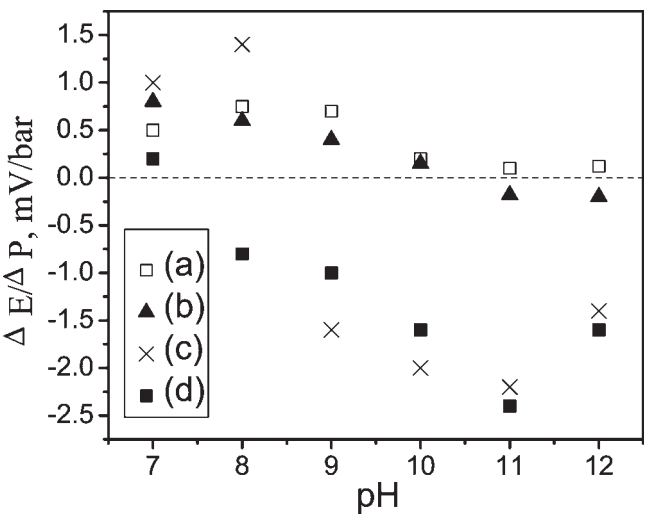

Figure 5 SP of (a) membrane A, (b) membrane B, (c) membrane C, and (d) membrane D.

From Figure 5, it can be seen that membrane D behaves positive SP value at pH = 7, then changes to negative values at pH = 8, indicating that the charge transition point of membrane D is at pH = 7–8. Similar changing of the SP value as the pH increases is also observed for membranes B and C and their charge transition point is at pH = 10–11 and pH = 8–9, respectively. For membrane A, no charge transition behavior is observed, which suggests that the charge transition point of membrane A is at pH > 12 or does not exit at all.

It has been researched that the charge transition point of alumina supports or membranes is at pH = 4–5 because the surfaces and pores of oxide ceramic materials are occupied by amphoteric MOH (M = Al, Si, etc.) groups which is a result of an exposure to water in either liquid or gaseous form.[30] The amphoteric MOH groups are enabled to dissociate when the surface and pores get in contact with polar liquids. This dissociation strongly depends on the pH of the solution and can be expressed by the following equations:[30]

$$\mathrm{MOH} + \mathrm{H^+} \rightarrow \mathrm{MOH_2^+} \leftrightarrow \mathrm{M^+} + \mathrm{H_2O} \quad (1)$$

$$\mathrm{MOH} + \mathrm{OH^-} \rightarrow \mathrm{M(OH)_2^-} \leftrightarrow \mathrm{MO^-} + \mathrm{H_2O} \quad (2)$$

For alumina supports or membranes, at pH higher than 5, mainly reaction (2) takes place and so negatively charged MO^- (AlO_2^-) are produced on the solid surfaces and pores. The amount of the produced AlO_2^- depends strongly on the pH value of the KCl solutions. After the dip-coating of the alumina supports in the coating solutions, hybrid layers form on the membranes. The final hybrid membranes thus contain positive charges, i.e., the quarteramine ($—N^+(CH_3)_3—$) groups. These groups can counteract the behavior of AlO_2^- groups, partly or wholly depending on their relative amount. From the measurements results of the hybrid membranes A–D in Figure 5, it can be seen that as the positive charge content increases from membranes D to A, this kind of counteracting effect strengthens. That is, at pH < 8, the $—N^+(CH_3)_3—$ groups of the membrane D can counteract the AlO_2^- groups of the substrate wholly. However, at pH = 8, the AlO_2^- groups increase, so the $—N^+(CH_3)_3—$ groups can only partly counteract the AlO_2^- groups and the membrane behaves negative SP values. For membrane C, B and A, the $—N^+(CH_3)_3—$ groups can wholly counteract the AlO_2^- groups at pH < 9, pH < 11 and pH as high as 12.

CONCLUSIONS

New positively charged organic–inorganic hybrid materials and membranes were prepared through the ring-opening and sol–gel processes of the GMA and γ-MPS copolymers. The molar ratio of GMA/γ-MPS varied from 83/17 to 35/65 so that four different hybrid materials (hybrid materials A–D) and membranes (membranes A–D) were obtained.

Characterizations showed that in the hybrid materials A–D, few epoxy and uncondensed —SiOH groups remained. The thermal degradation temperatures (T_d) of the hybrid materials were in the range of 223–251°C.

Hydrophilicity of the hybrid materials/membranes decreased as the γ-MPS content increased, as reflected by the gradually decreasing water uptake (W_R) and the increasing water contact angle. Also, as the γ-MPS content increased, IEC and the pure water flux decreased. Pore diameters of the hybrid membranes estimated from the water flux by the method described in our previous article[29] were in the range of 0.006–0.002 μm.

Another interesting point with these hybrid membranes was that from membranes A to D, the charge transition point, as determined from the SP behavior, decreased gradually from pH > 12 to pH = 7–8. This was mainly due to the synergism function of the AlO_2^- groups of the alumina substrates and the $—N^+(CH_3)_3—$ groups of the hybrid membranes.

References

1. Chen, J.; Chareonsak, R.; Puengpipat, V.; Marturunkakul, S. J Appl Polym Sci 1999, 74, 1341.
2. Nagarale, R. K.; Shahi, V. K.; Rangarajan, R. J Membr Sci 2005, 248, 37.
3. Hsu, Y. G.; Lin, F. J. J Appl Polym Sci 2000, 75, 275.
4. MacGibbon, R. M. A.; Badheka, R.; Sermon, P. A. J Sol-Gel Sci Technol 2004, 32, 53.
5. Zulfikar, M. A.; Mohammad, A. W.; Kadhum, A. A.; Hilal, N. J Appl Polym Sci 2006, 99, 3163.
6. Honma, I.; Hirakawa, S.; Yamada, K.; Bae, J. M. Solid State Ionics 1999, 118, 29.
7. Nakajima, H.; Honma, I. Solid State Ionics 2002, 148, 607.
8. Lu, Z. H.; Liu, G. J.; Duncan, S. J Membr Sci 2003, 221, 113.
9. Cornelius, C. J.; Marand, E. J Membr Sci 2002, 202, 97.
10. Hsiue, G. H.; Kuo, W. J.; Huang, Y. P.; Jeng, R. J. Polymer 2000, 41, 2813.
11. Lee, L. H.; Chen, W. C. Chem Mater 2001, 13, 1137.
12. Okada, A.; Usuki, A. Mater Sci Eng C 1995, 3, 109.
13. Gilman, J. W. Appl Clay Sci 1999, 15, 31.
14. Binsu, V. V.; Nagarale, R. K.; Shahi, V. K. J Mater Chem 2005, 15, 4823.
15. Wang, H. T.; Holmberg, B. A.; Huang, L. M. J Mater Chem 2002, 12, 834.
16. Walcarius, A. Chem Mater 2001, 13, 3351.
17. Wu, C. M.; Xu, T. W.; Yang, W. H. J Membr Sci 2003, 216, 269.
18. Wu, C. M.; Xu, T. W.; Yang, W. H. J Solid State Chem 2004, 177, 1660.
19. Wu, C. M.; Xu, T. W.; Gong, M.; Yang, W. H. J Membr Sci 2005, 247, 111.

20. Wu, C. M.; Xu, T. W.; Yang, W. H. Eur Polym J 2005, 41, 1901.
21. Zhang, S. L.; Xu, T. W.; Wu, C. M. J Membr Sci 2005, 269, 142.
22. Zhang, S. L.; Wu, C. M.; Xu, T. W.; Gong, M.; Xu, X. L. J Solid State Chem 2005, 178, 2292.
23. Mouanda, B. Polymer 1997, 38, 5301.
24. Schmid, G.; Schwarz, H. J Membr Sci 1998, 150, 197.
25. Rosu, D.; Cascaval, C. N.; Rosu, L. J Photochem Photobiol A 2006, 177, 218.
26. Toutorski, I. A.; Tkachenko, T. E.; Pokidko, B. V. J Sol-Gel Sci Technol 2003, 26, 505.
27. Bondar, Y.; Kim, H. J.; Yoon, S. H.; Lim, Y. J. React Funct Polym 2004, 58, 43.
28. Inaki, Y.; Yoshida, H.; Yoshida, T.; Hattori, T. J Phys Chem B 2002, 106, 9098.
29. Wu, C. M.; Xu, T. W.; Yang, W. H. J Membr Sci 2003, 224, 117.
30. Moritz, T.; Benfer, S.; Arki, P.; Tomandl, G. Colloids Surf A 2001, 47, 25.